Journal of Applied Analysis and Computation
Volume 13, Number 2, April 2023, 969–985
Website:http://www.jaac-online.com
DOI:10.11948/20220254

A SPACE-TIME SPECTRAL COLLOCATION METHOD FOR SOLVING THE VARIABLE-ORDER FRACTIONAL FOKKER-PLANCK EQUATION

Ahmed Z. Amin[1], António M. Lopes[2,†] and Ishak Hashim[1]

Abstract A numerical approach for solving the variable-order fractional Fokker-Planck equation (VO-FFPE) is proposed. The computational scheme is based on the shifted Legendre Gauss-Lobatto and the shifted Chebyshev Gauss-Radau collocation methods. The VO-FFPE is written as a truncated series of shifted Legendre and shifted Chebyshev polynomials for space and time variables, respectively. The residuals of the VO-FFPE at the shifted Legendre Gauss-Lobatto and shifted Chebyshev Gauss-Radau quadrature points are estimated. The original problem is converted into a system of algebraic equations that can be solved easily. Several examples are presented to demonstrate the efficacy of the technique.

Keywords Fractional calculus, Caputo fractional derivative of variable order, fractional Fokker-Planck equation, spectral collocation method.

MSC(2010) 65Mxx, 44Axx, 35Qxx.

1. Introduction

Fractional calculus (FC) [32, 34–36] is the branch of calculus that generalizes the concepts of derivative and integral to non-integer orders. The FC has become an active area of research and development in many fields of science [9,23,28,40], due to its suitability for describing a wide range of physical phenomena, involving diffusion and damping laws. Indeed, fractional derivatives are a powerful tool for modeling memory and heredity effects in a variety of materials and processes. Fractional differential equations (FDEs) [3,43,44] are well suited to a wide range of engineering and physics problems [13]. However, finding accurate techniques for solving FDEs is a demanding and motivating topic in engineering, physics, and mathematics, since most FDEs do not have exact or analytic solutions.

The Fokker-Planck equation [31,38] describes the time evolution of a probability density function. It is also known as the Kolmogorov forward equation. The Fokker-Planck equation was firstly used in the statistical description of the Brownian motion of a particle in a fluid. Fractional Fokker-Planck equations (FFPEs) [29,30,33] were then adopted to describe the Brownian motion of particles, to model the change of

†The corresponding author. Email: aml@fe.up.pt (A.M. Lopes)
[1]Department of Mathematical Sciences, Faculty of Science & Technology, Universiti Kebangsaan, 43600 UKM Bangi, Selangor, Malaysia
[2]LAETA/INEGI, Faculty of Engineering, University of Porto, Rua Dr Roberto Frias, 4200-465 Porto, Portugal

probability in time and space of random functions, and to model the transport of solutes [25,26,38], just to mention a few applications. Finding numerical solutions of FFPEs has received great interest recently, namely in stochastic dynamical systems. In [45] the Galerkin finite elements approach was proposed, in [21] the finite differences and the shifted Chebyshev collocation methods were adopted, in [41] the Chebyshev wavelet scheme was investigated, and in [22] the Jacobi collocation method was used, just to cite a few.

Several numerical methods for solving variable-order (VO) fractional differential equations (VO-FDEs) have been investigated. In [10] Bernstein polynomials were used to solve a linear VO fractional cable equation, in [4] a collocation method for solving a 2D nonlinear VO fractional cable equation was employed, and in [39] incorporating the Caputo derivative for solving VO-FDEs was suggested. Other numerical techniques can be found in [1,5,14,17,18,42].

A frequent objection against the use of one-step or multi-step methods for solving FDEs is that these methods are local. This seems to contradict the concepts underneath fractional operators, which are intrinsically non-local. One potential and promising approach in this direction is the use of spectral methods [13]. The spectral methods [11,12,16,27] have better accuracy than other numerical techniques and possess exponential rates of convergence [2,6,7,15,19,20]. Spectral techniques have been broadly utilized in several areas, with those that are dependent upon the Fourier expansion being applied to problems with periodic boundary conditions.

The contribution of this paper is to present a new scheme based on the shifted Legendre Gauss-Lobatto collocation (SL-GL-C) and shifted Chebyshev Gauss-Radau collocation (SC-GR-C) methods to solve the VO fractional Fokker-Planck equation (VO-FFPE) given by

$$D_\rho^{\delta(\xi,\rho)}\varphi(\xi,\rho) = \left[\chi_1(\xi)D_\xi^{2\sigma(\xi,\rho)} + \chi_2(\xi)D_\xi^{\sigma(\xi,\rho)}\right]\varphi(\xi,\rho) + \psi(\xi,\rho), \tag{1.1}$$

subject to the initial condition

$$\varphi(\xi,0) = \phi(\xi), \qquad \xi \in [0,L], \tag{1.2}$$

and boundary conditions

$$\varphi(0,\rho) = \omega_0(\rho), \qquad \varphi(L,\rho) = \omega_1(\rho), \qquad \rho = [0,T]. \tag{1.3}$$

The shifted Legendre Gauss-Lobatto (SL-GL) and shifted Chebyshev Gauss-Radau (SC-GR) points are used to approximate the solution of the VO-FFPE in space and time, respectively. The VO-FFPE is written as a truncated series of shifted Legendre polynomials (SLP) and shifted Chebyshev polynomials (SCP). The residuals of the VO-FFPE at the SL-GL and SC-GR quadrature points are estimated. Finally, a system of algebraic equations is obtained and solved. Numerical simulations are presented to verify the accuracy of the procedure.

The paper organization is as follows: Section 2 introduces preliminary concepts and recalls some properties of SLP and SCP. Section 3 is divided into two subsections: subsection 3.1 solves the space VO-FFPE (SVO-FFPE) with initial-value and boundary condition, while subsection 3.2 address the time-space VO-FFPE (TSVO-FFPE). Section 4 presents numerical examples to illustrate the performance and accuracy of the techniques. Section 5 draws the conclusions.

2. Mathematical preliminaries

2.1. Fractional calculus

We introduce some definitions [24,32,37] that are useful for the rest of the paper.

Definition 2.1 ([13,32]). The fractional integral (or Riemann-Liouville integral) of order $\sigma > 0$ of the function $\varphi(\xi)$, $\xi \in (a,b)$, is given by:

$$\begin{cases} (I^{\sigma}\varphi)(\xi) = \frac{1}{\Gamma(\sigma)} \displaystyle\int_0^{\xi} (\xi - s)^{\sigma-1}\varphi(s)ds, & \sigma > 0, \\ \varphi(\xi), & \sigma = 0. \end{cases} \tag{2.1}$$

Definition 2.2 ([24]). The left and right Riemann–Liouville derivatives of order $\sigma > 0$ of the function $\varphi(\xi)$, $\xi \in (a,b)$, are given by:

$$_{RL}D^{\sigma}_{a,\xi}\varphi(\xi) = \frac{d^m}{d\xi^m}\left[D^{-(m-\sigma)}_{a,\xi}\varphi(\xi)\right] \tag{2.2}$$

and

$$_{RL}D^{\sigma}_{\xi,b}\varphi(\xi) = (-1)^m \frac{d^m}{d\xi^m}\left[D^{-(m-\sigma)}_{\xi,b}\varphi(\xi)\right], \tag{2.3}$$

respectively, where m is a positive integer satisfying $m - 1 \leq \sigma < m$.

Definition 2.3 ([24]). The left and right Caputo derivatives of order $\sigma > 0$ of the function $\varphi(\xi)$, $\xi \in (a,b)$, are given by:

$$_{C}D^{\sigma}_{a,\xi}\varphi(\xi) = D^{-(m-\sigma)}_{a,\xi}\left[\varphi^{(m)}(\xi)\right] \tag{2.4}$$

and

$$_{C}D^{\sigma}_{\xi,b}\varphi(\xi) = (-1)^m D^{-(m-\sigma)}_{\xi,b}\left[\varphi^{(m)}(\xi)\right], \tag{2.5}$$

respectively, where m is a positive integer satisfying $m - 1 \leq \sigma < m$.

Definition 2.4 ([4]). The Caputo derivative of VO $\sigma(\xi,\rho)$ is defined as:

$$D^{\sigma(\xi,\rho)}_{\xi}\varphi(\xi,\rho) = \frac{1}{\Gamma(1-\sigma(\xi,\rho))}\int_0^{\xi}(\xi-\varepsilon)^{-\sigma(\xi,\rho)}\varphi^{(1)}(\varepsilon,\rho)d\varepsilon. \tag{2.6}$$

Definition 2.5 ([15]). The Riemann-Liouville fractional derivative of VO $\sigma(\xi,\rho)$ is defined by:

$$D^{\sigma(\xi,t)}_{\xi}\varphi(\xi,\rho) = \frac{1}{\Gamma(m-\sigma(\xi,t))}\frac{d^m}{dt^m}\int_0^{\xi}(\xi-\varepsilon)^{m-\sigma(\xi,t)-1}\varphi(\varepsilon,\rho)d\varepsilon. \tag{2.7}$$

2.2. Shifted Legendre polynomials

The Legendre polynomials $\mathcal{L}_{\gamma}(\xi)$, $\gamma = 0, 1 \ldots$, satisfy the Rodrigues formula

$$\mathcal{L}_{\gamma}(\xi) = \frac{(-1)^{\gamma}}{2^{\gamma}\gamma!}D^{\gamma}((1-\xi^2)^{\gamma}). \tag{2.8}$$

Also, $\mathcal{L}_\gamma(\xi)$ are polynomials of degree γ and, therefore, we get $\mathcal{L}_\gamma^{(p)}(\xi)$ (the pth derivative of $\mathcal{L}_\gamma(\xi)$) as

$$\mathcal{L}_\gamma^{(p)}(\xi) = \sum_{i=0(\gamma+\nu=even)}^{\gamma-p} C_p(\gamma,\nu)\mathcal{L}_\nu(\xi), \tag{2.9}$$

where

$$C_p(\gamma,\nu) = \frac{2^{p-1}(2\nu+1)\Gamma(\frac{p+\gamma-\nu}{2})\Gamma(\frac{p+\gamma+\nu+1}{2})}{\Gamma(p)\Gamma(\frac{2-p+\gamma-\nu}{2})\Gamma(\frac{3-p+\gamma+\nu}{2})}. \tag{2.10}$$

The Legendre polynomials satisfy the relations

$$\begin{cases} \mathcal{L}_0(\xi) = 1, \\ \mathcal{L}_1(\xi) = \xi, \\ \mathcal{L}_{\gamma+2}(\xi) = \dfrac{2\gamma+3}{\gamma+2}\xi\mathcal{L}_{\gamma+1}(\xi) - \dfrac{\gamma+1}{\gamma+2}\mathcal{L}_\gamma(\xi), \end{cases} \tag{2.11}$$

and we get the orthogonality by

$$(\mathcal{L}_\gamma(\xi), \mathcal{L}_l(\xi))_w = \int_{-1}^{1} \mathcal{L}_\gamma(\xi)\mathcal{L}_l(\xi)\, w(\xi) = h_\gamma \delta_{l\gamma}, \tag{2.12}$$

where $w(\xi)=1$, $h_\gamma = \frac{2}{2\gamma+1}$.

The Legendre Gauss-Lobatto quadrature has been used to evaluate the preceding integrals efficiently. For any $\psi \in S_{2\mu-1}[-1,1]$, we have

$$\int_{-1}^{1} \psi(\xi)d\xi = \sum_{\tau=0}^{\mu} \varpi_{\mu,\tau}\psi(\xi_{\mu,\tau}). \tag{2.13}$$

Let us introduce the discrete inner product as

$$(\psi,\varphi)_w = \sum_{\tau=0}^{\mu} \psi(\xi_{\mu,\tau})\,\varphi(\xi_{\mu,\tau})\,\varpi_{\mu,\tau}. \tag{2.14}$$

For the Legendre Gauss-Lobatto we find that $\xi_{\mu,0} = -1$, $\xi_{\mu,\mu} = 1$, $\xi_{\mu,\tau}(\tau = 1,\cdots,\mu-1)$ are the zeros of $(l_\mu(\xi))'$, and $\varpi_{\mu,\tau} = 2/\mu(\mu+1)(L_\mu(\xi_{\mu,\tau}))^2$, where $\xi_{\mu,\tau}$ $(0 \le \tau \le \mu)$ and $\varpi_{\mu,\tau}$ $(0 \le \tau \le \mu)$ are utilized as the nodes and the corresponding Christoffel numbers within $[-1,1]$, respectively ([8]). In order to adopt these polynomials in the interval $\xi \in (0,l_1)$ we define the so-called SLPs by using $\xi = 2\xi/l_1 - 1$.

We denote by $\mathcal{L}_{l_1,\nu}(\xi)$ the SLPs $\mathcal{L}_\nu\left(\dfrac{2\xi}{l_1}-1\right)$. Then, $\mathcal{L}_{l_1,\nu}(\xi)$ can be acquired as

$$(\nu+1)\mathcal{L}_{l_1,\nu+1}(\xi) = (2\nu+1)\left(\frac{2\xi}{l_1}-1\right)\mathcal{L}_{l_1,\nu}(\xi) - \nu\mathcal{L}_{l_1,\nu-1}(\xi), \qquad \nu = 1,2,\ldots. \tag{2.15}$$

The analytic form of the SLPs $\mathcal{L}_{l_1,\nu}(\xi)$ of degree ν is given by

$$\mathcal{L}_{l_1,\nu}(\xi) = \sum_{\gamma=0}^{\nu} (-1)^{\nu+\gamma}\frac{(\nu+\gamma)!}{(\nu-\gamma)!(\gamma!)^2\,L^\gamma}\xi^\gamma. \tag{2.16}$$

The expression of the orthogonality condition reads as

$$\int_0^l \mathcal{L}_{l_1,\tau}(\xi)\mathcal{L}_{l_1,\gamma}(\xi)w_{l_1}(\xi)d\xi = \hbar_\gamma\, \delta_{\tau\gamma}, \tag{2.17}$$

where $w_{l_1}(\xi) = 1$ and $\hbar_\gamma = l_1/(2\gamma+1)$.

A function $\psi(\xi)$, square integrable in $(0,l)$, may be expressed in terms of SLPs as

$$\psi(\xi) = \sum_{\tau=0}^{\infty} c_\tau \mathcal{L}_{l_1,\tau}(\xi), \tag{2.18}$$

and the coefficients c_τ are given by

$$c_\tau = \frac{1}{\hbar_\tau}\int_0^l \psi(\xi)\mathcal{L}_{l_1,\tau}(\xi)w_{l_1}(\xi)d\xi, \quad \tau = 0,1,2,\dots. \tag{2.19}$$

In practice, only the first $(\mu+1)$-terms of the SLPs are applied. Thus, $\varphi(\xi)$ is written as

$$\psi_\mu(\xi) \simeq \sum_{\tau=0}^{\mu} c_\tau \mathcal{L}_{l_1,\tau}(\xi). \tag{2.20}$$

2.3. Shifted Chebyshev polynomials

The Chebyshev polynomials are defined in $[-1,1]$ by [8]

$$\mathcal{T}_\tau(\rho) = \cos(\tau \arccos(\rho)), \quad \tau \geq 0. \tag{2.21}$$

Also,

$$\mathcal{T}_\tau(\pm 1) = (\pm 1)^\tau, \quad \mathcal{T}_\tau(-\rho) = (-1)^\tau \mathcal{T}_\tau(\rho). \tag{2.22}$$

Let us consider $w^c(\rho) = \dfrac{1}{\sqrt{1-\rho^2}}$. Then, we introduce the $L^2_{w^c}$ weighted space inner product and norm as

$$\|\varphi\|_{w^c} = (\varphi,\varphi)^{\frac{1}{2}}_{w^c}, \qquad (\varphi,\chi)_{w^c} = \int_{-1}^{1} \varphi(\rho)\,\chi(\rho) w^c(\rho)d\rho. \tag{2.23}$$

The set of Chebyshev polynomials satisfies

$$\|\mathcal{T}_\varrho\|^2_{w^c} = h^c_\varrho = \begin{cases} 0, & \varrho \neq \tau, \\ \dfrac{\gamma_\varrho}{2}\pi, & \varrho = \tau, \end{cases} \quad \gamma_0 = 2, \quad \gamma_\varrho = 1, \quad \varrho \geq 1. \tag{2.24}$$

Now, we define the norm and discrete inner product

$$\|\varphi\|_{w^c} = (\varphi,\varphi)^{\frac{1}{2}}_{w^c}, \qquad (\varphi,\chi)_{w^c} = \sum_{\tau=0}^{\kappa} \varphi(\varepsilon_{\kappa,\tau})\,\chi(\varepsilon_{\mu,\tau})\,\varpi^c_{\kappa,\tau}. \tag{2.25}$$

Let us denote by $\mathcal{T}_{L,\jmath}(\rho)$ the SCPs in $[0,L]$. The analytic form of $\mathcal{T}_{L,\jmath}(\rho)$ is acquired from

$$\mathcal{T}_{L,\jmath}(\rho) = n\sum_{\tau=0}^{\jmath} (-1)^{\jmath-\tau} \frac{(\jmath+\tau-1)!\; 2^{2\tau}}{(\jmath-\tau)!\; (2\tau)!\; L^\tau}\; \rho^\tau, \tag{2.26}$$

where $\mathcal{T}_{L,\jmath}(0) = (-1)^\jmath$ and $\mathcal{T}_{L,\jmath}(\rho) = 1$.

The orthogonality condition is

$$\int_0^L \mathcal{T}_{L,\jmath}(\rho)\mathcal{T}_{L,\tau}(\rho)W_L(\rho)d\rho = \delta_{\jmath\tau}\, h_\tau^L. \tag{2.27}$$

If $\varphi(\rho) \in L^2_{w_L(\rho)}[0, L]$, we can write

$$\varphi(\rho) = \sum_{\tau=0}^{\infty} e_\tau \mathcal{T}_{L,\tau}(\rho), \tag{2.28}$$

where

$$e_\tau = \frac{1}{{}^c h_\tau^T} \int_0^L \varphi(\rho)\mathcal{T}_{L,\tau}(\rho)W_L(\rho)d\rho, \quad \tau = 0, 1, 2, \ldots. \tag{2.29}$$

3. Numerical algorithm to solve VO-FFPEs

Our method uses the spectral collocation approximation by merging the SL-GL and SC-GR quadrature formulas for solving SVO-FFPEs and TSVO-FFPEs.

3.1. Space VO-FFPEs

Herein, we derive a numerical scheme for solving the SVO-FFPE

$$D_\rho\varphi(\xi, \rho) = \big[\chi_1(\xi)D_\xi^{2\sigma(\xi,\rho)} + \chi_2(\xi)D_\xi^{\sigma(\xi,\rho)}\big]\varphi(\xi, \rho) + \psi(\xi, \rho), \tag{3.1}$$

with initial condition

$$\varphi(\xi, 0) = \phi(\xi), \qquad \xi \in [0, L], \tag{3.2}$$

and boundary condition

$$\varphi(0, \rho) = \omega_0(\rho), \qquad \varphi(L, \rho) = \omega_1(\rho), \qquad \rho = [0, T], \tag{3.3}$$

where $\varphi(\xi, \rho)$ is unknown, the functions $\sigma(\xi, \rho)$, $\psi(\xi, \rho)$, $\chi_1(\xi)$, $\psi(\xi, \rho)\chi_2(\xi)$, $\phi(\xi)$, $\omega_0(\rho)$, $\omega_1(\rho)$ are well-known, and

$$\begin{aligned} D_\xi^{\sigma(\xi,\rho)}\varphi(\xi, \rho) &= \frac{1}{\Gamma(1 - \sigma(\xi, \rho))} \int_0^\xi (\xi - \upsilon)^{-\sigma(\xi,\rho)}\varphi^{(1)}(\upsilon, \rho)d\upsilon, \\ D_\xi^{2\sigma(\xi,\rho)}\varphi(\xi, \rho) &= \frac{1}{\Gamma(2 - 2\sigma(\xi, \rho))} \int_0^\xi (\xi - \upsilon)^{-2\sigma(\xi,\rho)-1}\varphi^{(2)}(\upsilon, \rho)d\upsilon, \end{aligned} \tag{3.4}$$

are the space-fractional derivatives of $\varphi(\xi, \rho)$.

We use the SL-GL points and the SC-GR points [8] for space and time approximations, respectively. In the follow-up, we outline the primary steps for solving SVO-FFPEs.

We denote by $\varphi_{\text{Approx}}(\xi, \rho)$ the approximate solution of (3.1), yielding

$$\varphi_{\text{Approx}}(\xi, \rho) = \sum_{\gamma=0}^{\mu}\sum_{\tau=0}^{\kappa} e_{\gamma,\tau}\mathcal{L}_{L,\gamma}(\xi)\mathcal{T}_{T,\tau}, \tag{3.5}$$

and we compute the time partial derivative $D_\rho\varphi(\xi,\rho)$ as

$$D_\rho\varphi(\xi,\rho)=\sum_{\gamma=0}^{\mu}\sum_{\tau=0}^{\kappa}e_{\gamma,\tau}\mathcal{L}_{L,\gamma}(\xi)D_\rho\mathcal{T}_{T,\tau}=\sum_{\gamma=0}^{\mu}\sum_{\tau=0}^{\kappa}e_{\gamma,\tau}\eta_1^{\gamma,\tau}(\xi,\rho), \tag{3.6}$$

where $\eta_1^{\gamma,\tau}(\xi,\rho)=\mathcal{L}_{L,\gamma}(\xi)D_\rho\mathcal{T}_{T,\tau}(\rho)$.

Also, we approximate the terms on the right-hand-side of (3.1) as

$$\begin{aligned}D_\xi^{\sigma(\xi,\rho)}\varphi(\xi,\rho)&=\sum_{\gamma=0}^{\mu}\sum_{\tau=0}^{\kappa}e_{\gamma,\tau}\eta_2^{\gamma,\tau}(\xi,\rho),\\ D_\xi^{2\sigma(\xi,\rho)}\varphi(\xi,\rho)&=\sum_{\gamma=0}^{\mu}\sum_{\tau=0}^{\kappa}e_{\gamma,\tau}\eta_3^{\gamma,\tau}(\xi,\rho),\end{aligned} \tag{3.7}$$

where $\eta_2^{\gamma,\tau}(\xi,\rho)=D_\xi^{\sigma(\xi,\rho)}\mathcal{L}_{L,\gamma}(\xi)\mathcal{T}_{T,\tau}(\rho)$ and $\eta_3^{\gamma,\tau}(\xi,\rho)=D_\xi^{2\sigma(\xi,\rho)}\mathcal{L}_{L,\gamma}(\xi)\mathcal{T}_{T,\tau}(\rho)$.

Therefore, adopting Eqs. (3.5)–(3.7), we rewrite (3.1) as

$$\begin{aligned}\sum_{\gamma=0}^{\mu}\sum_{\tau=0}^{\kappa}e_{\gamma,\tau}\eta_1^{\gamma,\tau}(\xi,\rho)=&\chi_1(\xi)\sum_{\gamma=0}^{\mu}\sum_{\tau=0}^{\kappa}e_{\gamma,\tau}\eta_2^{\gamma,\tau}(\xi,\rho)\\ &+\chi_2(\xi)\sum_{\gamma=0}^{\mu}\sum_{\tau=0}^{\kappa}e_{\gamma,\tau}\eta_3^{\gamma,\tau}(\xi,\rho)+\psi(\xi,\rho),\end{aligned} \tag{3.8}$$

for $(\xi,\rho)\in[0,L]\times[0,T]$. We can rewrite the initial and boundary conditions as

$$\begin{cases}\varphi(\xi,0)=\sum_{\gamma=0}^{\mu}\sum_{\tau=0}^{\kappa}e_{\gamma,\tau}\mathcal{L}_{L,\gamma}(\xi)\mathcal{T}_{T,\tau}(0)=\phi(\xi),\\ \varphi(0,\rho)=\sum_{\gamma=0}^{\mu}\sum_{\tau=0}^{\kappa}e_{\gamma,\tau}\mathcal{L}_{L,\gamma}(0)\mathcal{T}_{T,\tau}(\rho)=\omega_0(\rho),\\ \varphi(L,\rho)=\sum_{\gamma=0}^{\mu}\sum_{\tau=0}^{\kappa}e_{\gamma,\tau}\mathcal{L}_{L,\gamma}(L)\mathcal{T}_{T,\tau}(\rho)=\omega_1(\rho).\end{cases} \tag{3.9}$$

By applying the proposed SL-GL-C and SC-GR-C technique, and setting the residual of (3.1) equal to zero at $(\mu-1)\kappa$ collocation nodes, we have $\kappa(\mu-1)$ algebraic equations for $(\mu+1)(\kappa)$ unknowns $e_{\gamma,\tau}$,

$$\begin{aligned}&\sum_{\gamma=0}^{\mu}\sum_{\tau=0}^{\kappa}e_{\gamma,\tau}\eta_1^{\gamma,\tau}(\xi_{L,\mu,r},\rho_{T,\kappa,s})\\ =&\chi_1(\xi_{L,\mu,r})\sum_{\gamma=0}^{\mu}\sum_{\tau=0}^{\kappa}e_{\gamma,\tau}\eta_2^{\gamma,\tau}(\xi_{L,\mu,r},\rho_{T,\kappa,s})\\ &+\chi_2(\xi_{L,\mu,r})\sum_{\gamma=0}^{\mu}\sum_{\tau=0}^{\kappa}e_{\gamma,\tau}\eta_3^{\gamma,\tau}(\xi_{L,\mu,r},\rho_{T,\kappa,s})+\psi(\xi_{L,\mu,r},\rho_{T,\kappa,s}),\end{aligned} \tag{3.10}$$

for $r=1,\ldots,\mu-1$ and $s=1,\ldots,\kappa$. The initial and boundary conditions now become

$$\begin{cases} \sum_{\gamma=0}^{\mu}\sum_{\tau=0}^{\kappa} e_{\gamma,\tau}\mathcal{L}_{L,\gamma}(\xi_{L,\mu,r})\mathcal{T}_{T,\tau}(0) = \phi(\xi_{L,\mu,r}), \qquad r = 1,\dots,\mu-1, \\ \sum_{\gamma=0}^{\mu}\sum_{\tau=0}^{\kappa} e_{\gamma,\tau}\mathcal{L}_{L,\gamma}(0)\mathcal{T}_{T,\tau}(\rho_{T,\kappa,s}) = \omega_0(\rho_{T,\kappa,s}), \qquad s = 0,\dots,\kappa, \\ \sum_{\gamma=0}^{\mu}\sum_{\tau=0}^{\kappa} e_{\gamma,\tau}\mathcal{L}_{L,\gamma}(L)\mathcal{T}_{T,\tau}(\rho_{T,\kappa,s}) = \omega_1(\rho_{T,\kappa,s}) \qquad s = 0,\dots,\kappa, \end{cases} \tag{3.11}$$

and combining Eq.(3.10) and (3.11), we get

$$\begin{cases} \quad \sum_{\gamma=0}^{\mu}\sum_{\tau=0}^{\kappa} e_{\gamma,\tau}\eta_1^{\gamma,\tau}(\xi_{L,\mu,r},\rho_{T,\kappa,s}) \\ = \chi_1(\xi_{L,\mu,r})\sum_{\gamma=0}^{\mu}\sum_{\tau=0}^{\kappa} e_{\gamma,\tau}\eta_2^{\gamma,\tau}(\xi_{L,\mu,r},\rho_{T,\kappa,s}) \\ + \chi_2(\xi_{L,\mu,r})\sum_{\gamma=0}^{\mu}\sum_{\tau=0}^{\kappa} e_{\gamma,\tau}\eta_3^{\gamma,\tau}(\xi_{L,\mu,r},\rho_{T,\kappa,s}) + \psi(\xi_{L,\mu,r},\rho_{T,\kappa,s}), \\ \quad r = 1,\dots,\mu-1,\ s = 1,\dots,\kappa, \\ \sum_{\gamma=0}^{\mu}\sum_{\tau=0}^{\kappa} e_{\gamma,\tau}\mathcal{L}_{L,\gamma}(\xi_{L,\mu,r})\mathcal{T}_{T,\tau}(0) = \phi(\xi_{L,\mu,r}), \qquad r = 1,\dots,\mu-1, \\ \sum_{\gamma=0}^{\mu}\sum_{\tau=0}^{\kappa} e_{\gamma,\tau}\mathcal{L}_{L,\gamma}(0)\mathcal{T}_{T,\tau}(\rho_{T,\kappa,s}) = \omega_0(\rho_{T,\kappa,s}), \qquad s = 0,\dots,\kappa, \\ \sum_{\gamma=0}^{\mu}\sum_{\tau=0}^{\kappa} e_{\gamma,\tau}\mathcal{L}_{L,\gamma}(L)\mathcal{T}_{T,\tau}(\rho_{T,\kappa,s}) = \omega_1(\rho_{T,\kappa,s}) \qquad s = 0,\dots,\kappa. \end{cases} \tag{3.12}$$

Finally, the previous system of $(\mu+1)$ algebraic equations can be solved. As a result, $\varphi_{\text{Approx}}(\xi,\rho)$ can be calculated.

3.2. Time-space VO-FFPEs

Now, we extend the preceding technique to the TSVO-FFPE

$$D_\rho^{\delta(\xi,\rho)}\varphi(\xi,\rho) = \left[\chi_1(\xi)D_\xi^{2\sigma(\xi,\rho)} + \chi_2(\xi)D_\xi^{\sigma(\xi,\rho)}\right]\varphi(\xi,\rho) + \psi(\xi,\rho), \tag{3.13}$$

subject to the initial condition (3.2) and boundary conditions (3.3).

We compute the time partial derivative $D_\rho^{\delta}\varphi(\xi,\rho)$ as

$$D_\rho^{\delta(\xi,\rho)}\varphi(\xi,\rho) = \sum_{\gamma=0}^{\mu}\sum_{\tau=0}^{\kappa} e_{\gamma,\tau}\mathcal{L}_{L,\gamma}(\xi)D_\rho^{\delta(\xi,\rho)}\mathcal{T}_{T,\tau} = \sum_{\gamma=0}^{\mu}\sum_{\tau=0}^{\kappa} e_{\gamma,\tau}\eta_4^{\gamma,\tau}(\xi,\rho), \tag{3.14}$$

where $\eta_4^{\gamma,\tau}(\xi,\rho) = \mathcal{L}_{L,\gamma}(\xi)D_\rho^{\delta(\xi,\rho)}\mathcal{T}_{T,\tau}(\rho)$.

Following the steps provided in the preceding subsection and using Eqs. (3.5), (3.7) and (3.14), we obtain

$$\sum_{\gamma=0}^{\mu}\sum_{\tau=0}^{\kappa} e_{\gamma,\tau}\eta_4^{\gamma,\tau}(\xi,\rho) = \chi_1(\xi)\sum_{\gamma=0}^{\mu}\sum_{\tau=0}^{\kappa} e_{\gamma,\tau}\eta_2^{\gamma,\tau}(\xi,\rho)$$

$$+ \chi_2(\xi) \sum_{\gamma=0}^{\mu} \sum_{\tau=0}^{\kappa} e_{\gamma,\tau} \eta_3^{\gamma,\tau}(\xi, \rho) + \psi(\xi, \rho), \tag{3.15}$$

for $(\xi, \rho) \in [0, L] \times [0, T]$. We approximate Eq. (3.15) at $\kappa(\mu - 1)$ points as

$$\begin{aligned}
&\sum_{\gamma=0}^{\mu} \sum_{\tau=0}^{\kappa} e_{\gamma,\tau} \eta_4^{\gamma,\tau}(\xi_{L,\mu,r}, \rho_{T,\kappa,s}) \\
=&\chi_1(\xi_{L,\mu,r}) \sum_{\gamma=0}^{\mu} \sum_{\tau=0}^{\kappa} e_{\gamma,\tau} \eta_2^{\gamma,\tau}(\xi_{L,\mu,r}, \rho_{T,\kappa,s}) \\
&+ \chi_2(\xi_{L,\mu,r}) \sum_{\gamma=0}^{\mu} \sum_{\tau=0}^{\kappa} e_{\gamma,\tau} \eta_3^{\gamma,\tau}(\xi_{L,\mu,r}, \rho_{T,\kappa,s}) + \psi(\xi_{L,\mu,r}, \rho_{T,\kappa,s}),
\end{aligned} \tag{3.16}$$

for $r = 1, \ldots, \mu - 1$ and $s = 1, \ldots, \kappa$. By utilizing Eqs. (3.11) and (3.16) we obtain

$$\begin{cases}
\displaystyle\sum_{\gamma=0}^{\mu} \sum_{\tau=0}^{\kappa} e_{\gamma,\tau} \eta_4^{\gamma,\tau}(\xi_{L,\mu,r}, \rho_{T,\kappa,s}) \\
\displaystyle= \chi_1(\xi_{L,\mu,r}) \sum_{\gamma=0}^{\mu} \sum_{\tau=0}^{\kappa} e_{\gamma,\tau} \eta_2^{\gamma,\tau}(\xi_{L,\mu,r}, \rho_{T,\kappa,s}) \\
\displaystyle\quad + \chi_2(\xi_{L,\mu,r}) \sum_{\gamma=0}^{\mu} \sum_{\tau=0}^{\kappa} e_{\gamma,\tau} \eta_3^{\gamma,\tau}(\xi_{L,\mu,r}, \rho_{T,\kappa,s}) + \psi(\xi_{L,\mu,r}, \rho_{T,\kappa,s}), \\
qr = 1, \ldots, \mu - 1,\ s = 1, \ldots, \kappa, \\
\displaystyle\sum_{\gamma=0}^{\mu} \sum_{\tau=0}^{\kappa} e_{\gamma,\tau} \mathcal{L}_{L,\gamma}(\xi_{L,\mu,r}) \mathcal{T}_{T,\tau}(0) = \phi(\xi_{L,\mu,r}), \qquad r = 1, \ldots, \mu - 1, \\
\displaystyle\sum_{\gamma=0}^{\mu} \sum_{\tau=0}^{\kappa} e_{\gamma,\tau} \mathcal{L}_{L,\gamma}(0) \mathcal{T}_{T,\tau}(\rho_{T,\kappa,s}) = \omega_0(\rho_{T,\kappa,s}), \qquad s = 0, \ldots, \kappa, \\
\displaystyle\sum_{\gamma=0}^{\mu} \sum_{\tau=0}^{\kappa} e_{\gamma,\tau} \mathcal{L}_{L,\gamma}(L) \mathcal{T}_{T,\tau}(\rho_{T,\kappa,s}) = \omega_1(\rho_{T,\kappa,s}) \qquad s = 0, \ldots, \kappa.
\end{cases} \tag{3.17}$$

4. Numerical results

We solve several examples to verify the effectiveness and accuracy of the proposed methodology.

We define the absolute error (AE) as

$$AE(\xi, \rho) = |\varphi(\xi, \rho) - \varphi_{\text{Approx}}(\xi, \rho)|, \tag{4.1}$$

where $\varphi(\xi, \rho)$ and $\varphi_{\text{Approx}}(\xi, \rho)$ are the exact and approximate solutions at point ξ, ρ, respectively. The maximum absolute error (MAE) is calculated as

$$MAE = \max\{AE(\xi, \rho)\}. \tag{4.2}$$

Example 4.1. Consider the SVO-FFPE

$$\begin{cases} \dfrac{\partial\varphi(\xi,\rho)}{\partial\rho} = \big[-\xi\dfrac{\partial^{\sigma(\xi,\rho)}}{\partial\xi^{\sigma(\xi,\rho)}} + \dfrac{\xi^2}{2}\dfrac{\partial^{2\sigma(\xi,\rho)}}{\partial\xi^{2\sigma(\xi,\rho)}}\big]\varphi(\xi,\rho) + \psi(\xi,\rho), \\ \varphi(0,\rho) = 0, \ \varphi(3,\rho) = 3e^{\rho}, \\ \varphi(\xi,0) = \xi, \end{cases} \tag{4.3}$$

and $\psi(\xi,\rho)$ is given from the exact solution $\varphi(\xi,\rho) = \xi e^{\rho}$.

Applying our algorithm to this example we get the absolute errors shown in Table 1, for $\sigma(\xi,\rho) = \frac{6+\sin(\xi)}{4}$ and $\sigma(\xi,\rho) = \frac{7+\xi\cos(\xi)}{3}$, and $\mu = \kappa = 12$. Table 2 lists the respective MAE at various values of μ and κ. Fig. 1, and 2 represents ξ and ρ direction curve of the AE of Ex.4.1 for $\mu = \kappa = 12$, and $\sigma(\xi,\rho) = \frac{6+\sin(\xi)}{4}$. Fig. 3 we represent the logarithmic of the MAE ($\log_{10} MAE$) versus μ and κ. In Table 3 we compare our method with the approach presented in [22], in terms of the MAE. From the results, we verify that our scheme reveals superior accuracy, even for just a few points.

Table 1. The AE of EX. 4.1 for $\sigma(\xi,\rho) = \frac{6+\sin(\xi)}{4}$ and $\sigma(\xi,\rho) = \frac{7+\xi\cos(\xi)}{3}$, and $\mu = \kappa = 12$.

$\sigma(\xi,\rho)$	$\frac{6+\sin(\xi)}{4}$	$\frac{7+\xi\cos(\xi)}{3}$
$(0,0)$	6.29307×10^{-17}	1.37663×10^{-16}
$(0.2,0.2)$	1.03274×10^{-16}	1.77047×10^{-15}
$(0.4,0,4)$	8.72077×10^{-16}	3.21823×10^{-14}
$(0.6,0.6)$	9.1076×10^{-16}	8.02812×10^{-15}
$(0.8,0.8)$	1.3219×10^{-15}	1.5338×10^{-14}
$(1.0,1.0)$	1.67408×10^{-16}	2.30909×10^{-16}

Table 2. The MAE of Ex.4.1 for $\sigma(\xi,\rho) = \frac{6+\sin(\xi)}{4}$ and $\sigma(\xi,\rho) = \frac{7+\xi\cos(\xi)}{3}$, at several values of μ and κ.

$\sigma(\xi,\rho)$	$\mu=\kappa=2$	$\mu=\kappa=4$	$\mu=\kappa=6$	$\mu=\kappa=8$	$\mu=\kappa=10$	$\mu=\kappa=12$
$\frac{6+\sin(\xi)}{4}$	9.4×10^{-2}	5.7×10^{-5}	8.3×10^{-8}	7.2×10^{-11}	4.0×10^{-14}	3.6×10^{-15}
$\frac{7+\xi\cos(\xi)}{3}$	7.5×10^{-3}	7.2×10^{-5}	5.5×10^{-6}	1.7×10^{-10}	1.2×10^{-13}	9.3×10^{-14}

Table 3. The MAE of Ex.4.1 obtained with our method and with the approach reported in [22].

	Our Method			Method in [22]		
σ	$\mu=\kappa=8$	$\mu=\kappa=10$	$\mu=\kappa=12$	$\mu=\kappa=8$	$\mu=\kappa=12$	$\mu=\kappa=16$
0.5	7.2×10^{-11}	4.0×10^{-14}	3.6×10^{-15}	7.3×10^{-4}	2.1×10^{-7}	$3.6\times2.7\times10^{-11}$

Example 4.2. We consider the TSVO-FFPE

$$\begin{cases} \dfrac{\partial^{\delta(\xi,\rho)}\varphi(\xi,\rho)}{\partial\rho} = \big[-\dfrac{\xi}{6}\dfrac{\partial^{\sigma(\xi,\rho)}}{\partial\xi^{\sigma(\xi,\rho)}} + \dfrac{\xi^2}{12}\dfrac{\partial^{2\sigma(\xi,\rho)}}{\partial\xi^{2\sigma(\xi,\rho)}}\big]\varphi(\xi,\rho) + \psi(\xi,\rho), \\ \varphi(0,\rho) = 0, \ \varphi(1,\rho) = \rho, \\ \varphi(\xi,0) = 0, \end{cases} \tag{4.4}$$

and $\psi(\xi,\rho)$ is given from the exact solution $\varphi(\xi,\rho) = \xi^2\rho$.

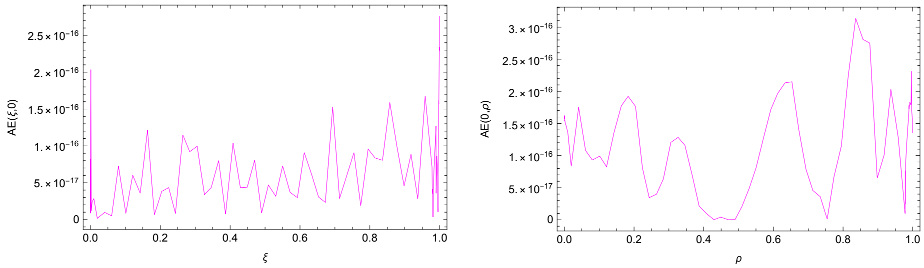

Figure 1. ξ and ρ direction curve of the AE of Ex.4.1 for $\mu = \kappa = 12$, $\sigma(\xi, \rho) = \frac{6+\sin(\xi)}{4}$.

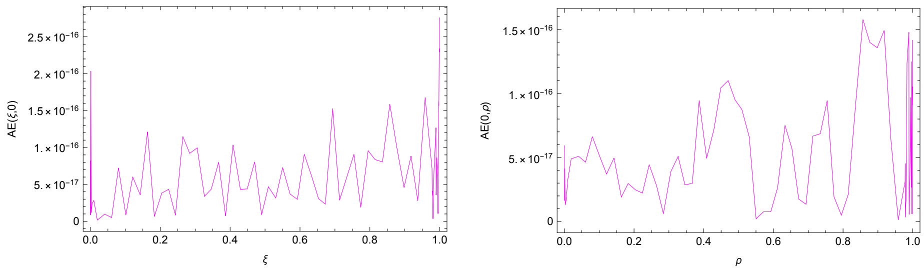

Figure 2. ξ and ρ direction curve of the AE of Ex.4.1 for $\mu = \kappa = 12$, $\sigma(\xi, \rho) = \frac{7+\xi\cos(\xi)}{3}$.

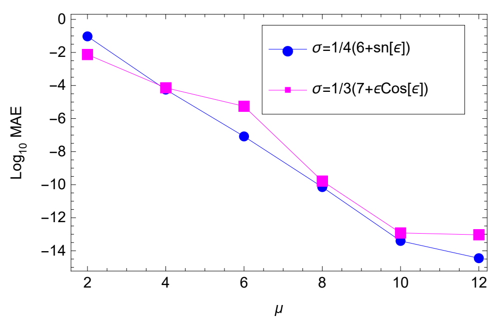

Figure 3. The $\log_{10} MAE$ versus μ of Ex.4.1 for $\sigma(\xi, \rho) = \frac{6+\sin(\xi)}{4}$ and $\sigma(\xi, \rho) = \frac{7+\xi\cos(\xi)}{3}$.

Table 4 shows the AE for $\sigma(\xi, \rho) = \frac{6+\xi\sin^2(\xi)}{4}$ and $\sigma(\xi, \rho) = \frac{6+\xi\cos^2(\xi)}{4}$, when $\delta(\xi, \rho) = \xi\sin(\rho)$ and $\mu = \kappa = 14$. Fig. 4 presents the The AE of Ex.4.2 for $\sigma(\xi, \rho) = \frac{6+\xi\sin^2(\xi)}{4}$ and $\sigma(\xi, \rho) = \frac{6+\xi\cos^2(\xi)}{4}$, when $\delta(\xi, \rho) = \xi\sin(\rho)$ and $\mu = \kappa = 14$. Again, the effectiveness of the proposed approach is well illustrated.

Example 4.3. Consider the TSVO-FFPE

$$\begin{cases} \dfrac{\partial^{\delta(\xi,\rho)}\varphi(\xi,\rho)}{\partial\rho} = \Big[-\dfrac{\xi}{6}\dfrac{\partial^{\sigma(\xi,\rho)}}{\partial\xi^{\sigma(\xi,\rho)}} + \dfrac{\xi^2}{12}\dfrac{\partial^{2\sigma(\xi,\rho)}}{\partial\xi^{2\sigma(\xi,\rho)}}\Big]\varphi(\xi,\rho) + \psi(\xi,\rho), \\ \varphi(0,\rho) = 0, \ \varphi(1,\rho) = \rho^2\sin(1), \\ \varphi(\xi,0) = \xi, \end{cases} \tag{4.5}$$

and $\psi(\xi, \rho)$ is given from the exact solution $\varphi(\xi, \rho) = \rho\sin(\xi)$.

Table 5 presents the MAE for $\sigma(\xi, \rho) = \frac{3+\sin(\xi)}{7}$, $\delta(\xi, \rho) = \xi^3\sin(\rho)$ and several values of μ and κ. Fig. 5 we represent ξ and ρ direction curve of the AE of Ex.4.3

Table 4. The AE of Ex.4.2 for $\sigma(\xi,\rho)=\frac{6+\xi\sin^2(\xi)}{4}$ and $\sigma(\xi,\rho)=\frac{6+\xi\cos^2(\xi)}{4}$, when $\delta(\xi,\rho)=\xi\sin(\rho)$ and $\mu=\kappa=14$.

$\sigma(\xi,\rho)$	$\frac{6+\xi\sin^2(\xi)}{4}$	$\frac{6+\xi\cos^2(\xi)}{4}$
$(0.1,0.1)$	$2,8381\times10^{-17}$	6.5204×10^{-17}
$(0.3,0.3)$	9.8862×10^{-17}	6.4085×10^{-17}
$(0.5,0,5)$	1.7144×10^{-17}	9.0250×10^{-18}
$(0.7,0.7)$	2.5633×10^{-17}	4.6364×10^{-17}
$(0.9,0.9)$	2.0467×10^{-17}	5.0805×10^{-17}

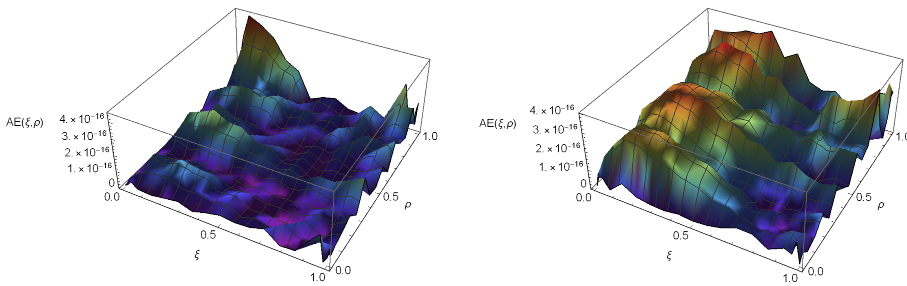

Figure 4. The AE versus ξ and ρ of Ex.4.2 for $\sigma(\xi,\rho)=\frac{6+\xi\sin^2(\xi)}{4}$ and $\sigma(\xi,\rho)=\frac{6+\xi\cos^2(\xi)}{4}$, when $\delta(\xi,\rho)=\xi\sin(\rho)$ and $\mu=\kappa=14$.

for $\sigma(\xi,\rho)=\frac{3+\sin(\xi)}{7}$, $\delta(\xi,\rho)=\xi^3\sin(\rho)$ and $\mu=\kappa=12$. Fig. 6 illustrates the proximity between $\varphi_{\text{Approx}}(\xi,\rho)$ and $\varphi(\xi,\rho)$ for $\mu=\kappa=12$. Fig. 7 represent the AE versus ξ and ρ of Ex.4.3 for $\sigma(\xi,\rho)=\frac{3+\sin(\xi)}{7}$, $\delta(\xi,\rho)=\xi^3\sin(\rho)$ and $\mu=\kappa=12$.

Table 5. The MAE of Ex.4.3 for $\sigma(\xi,\rho)=\frac{3+\sin(\xi)}{7}$ and $\delta(\xi,\rho)=\xi^3\sin(\rho)$.

$\sigma(\xi,\rho)$	$\mu=\kappa=2$	$\mu=\kappa=4$	$\mu=\kappa=6$	$\mu=\kappa=8$	$\mu=\kappa=10$	$\mu=\kappa=12$
$\frac{3+\sin(\xi)}{7}$	1.77×10^{-4}	1.45×10^{-5}	2.63×10^{-8}	2.14×10^{-11}	1.14×10^{-14}	3.75×10^{-16}

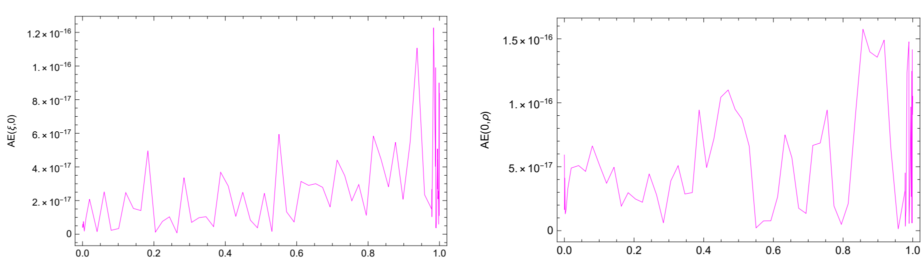

Figure 5. ξ and ρ direction curve of the AE of Ex.4.3 for $\sigma(\xi,\rho)=\frac{3+\sin(\xi)}{7}$, $\delta(\xi,\rho)=\xi^3\sin(\rho)$ and $\mu=\kappa=12$.

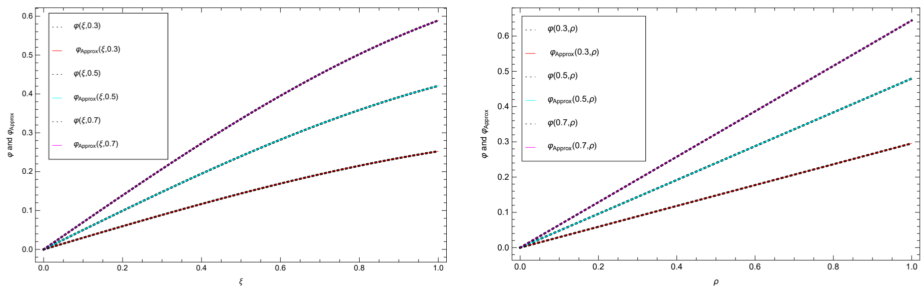

Figure 6. The $\varphi_{\text{Approx}}(\xi,\rho)$ and $\varphi(\xi,\rho)$ of Ex.4.3 for $\sigma(\xi,\rho)=\frac{3+\sin(\xi)}{7}$, $\delta(\xi,\rho)=\xi^3\sin(\rho)$ and $\mu=\kappa=12$.

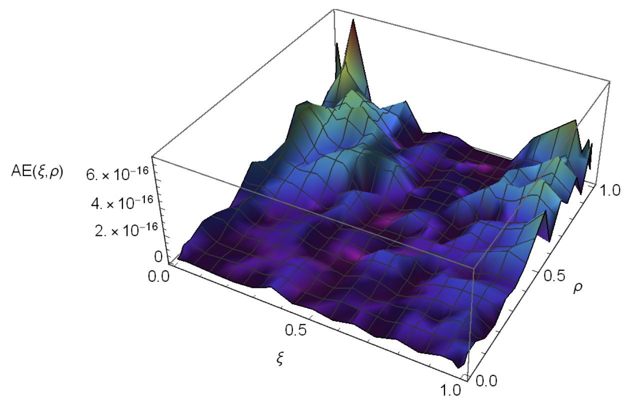

Figure 7. The AE versus ξ and ρ of Ex.4.3 for $\sigma(\xi,\rho)=\frac{3+\sin(\xi)}{7}$, $\delta(\xi,\rho)=\xi^3\sin(\rho)$ and $\mu=\kappa=12$.

Example 4.4. Consider the TSVO-FFPE

$$\begin{cases} \dfrac{\partial^{\delta(\xi,\rho)}\varphi(\xi,\rho)}{\partial\rho}=\big[-\xi\dfrac{\partial^{\sigma(\xi,\rho)}}{\partial\xi^{\sigma(\xi,\rho)}}+\dfrac{\xi^2}{2}\dfrac{\partial^{2\sigma(\xi,\rho)}}{\partial\xi^{2\sigma(\xi,\rho)}}\big]\varphi(\xi,\rho)+\psi(\xi,\rho), \\ \varphi(0,\rho)=0,\ \varphi(1,\rho)=\rho\sin(1), \\ \varphi(\xi,0)=\xi, \end{cases} \tag{4.6}$$

and $\psi(\xi,\rho)$ is obtained from the exact solution $\varphi(\xi,\rho)=\rho^2\sin(\xi)$.

Table 6 gives the MAE for $\sigma(\xi,\rho)=\frac{7+\xi^3\sin^2(\xi)}{9}$, $\delta(\xi,\rho)=\xi^2\sin(\rho)$ and several values of μ and κ. Fig. 8 compare $\varphi_{\text{Approx}}(\xi,\rho)$ and $\varphi(\xi,\rho)$ of Ex.4.4 for $\sigma(\xi,\rho)=\frac{7+\xi^3\sin^2(\xi)}{9}$, $\delta(\xi,\rho)=\xi^2\sin(\rho)$ and $\mu=\kappa=14$. Fig. 9 The AE of Ex.4.4 for $\sigma(\xi,\rho)=\frac{7+\xi^3\sin^2(\xi)}{9}$, $\delta(\xi,\rho)=\xi^2\sin(\rho)$ and $\mu=\kappa=14$. Fig. 10 plots the $\log_{10}MAE$, illustrating the exponential convergence of our algorithm for diverse values of μ. This shows that the suggested strategy produces accurate approximations and good convergence rates.

Table 6. The MAE of Ex.4.4 for $\sigma(\xi,\rho)=\frac{7+\xi^3\sin^2(\xi)}{9}$ and $\delta(\xi,\rho)=\xi^2\sin(\rho)$.

$\sigma(\xi,\rho)$	$\mu=\kappa=2$	$\mu=\kappa=4$	$\mu=\kappa=6$	$\mu=\kappa=8$	$\mu=\kappa=10$	$\mu=\kappa=12$	$\mu=\kappa=14$
$\frac{7+\xi^3\sin^2\xi}{9}$	2.6×10^{-3}	8.2×10^{-6}	2.2×10^{-8}	2.6×10^{-11}	1.5×10^{-14}	6.7×10^{-16}	4.5×10^{-16}

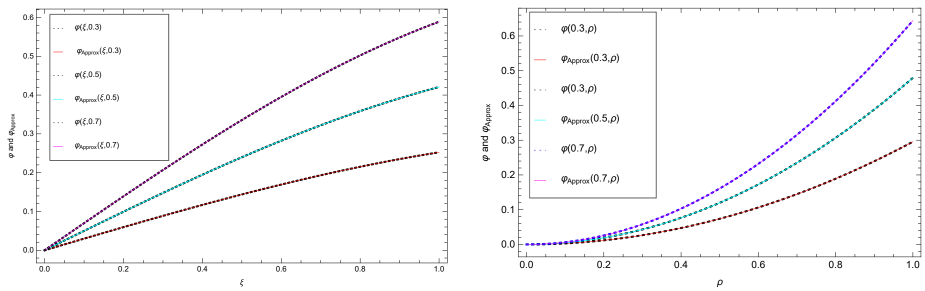

Figure 8. The $\varphi_{\text{Approx}}(\xi,\rho)$ and $\varphi(\xi,\rho)$ of Ex.4.4 for $\sigma(\xi,\rho)=\frac{7+\xi^3\sin^2(\xi)}{9}$, $\delta(\xi,\rho)=\xi^2\sin(\rho)$ and $\mu=\kappa=14$.

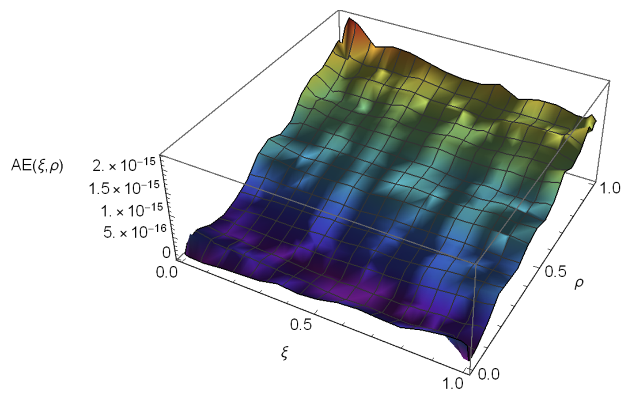

Figure 9. The AE of Ex.4.4 for $\sigma(\xi,\rho)=\frac{7+\xi^3\sin^2(\xi)}{9}$, $\delta(\xi,\rho)=\xi^2\sin(\rho)$ and $\mu=\kappa=14$.

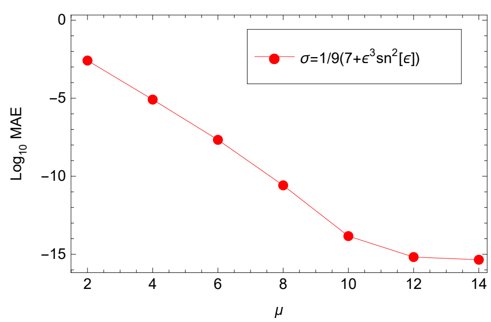

Figure 10. The $\log_{10} MAE$ versus μ of Ex.4.4 for $\sigma(\xi,\rho)=\frac{7+\xi^3\sin^2(\xi)}{9}$, $\delta(\xi,\rho)=\xi^2\sin(\rho)$.

5. Conclusion

In this paper, we introduced a new numerical technique for solving VO-FFPEs. The numerical scheme relies on the SL-GL-C and SC-GR-C methods, where the SL-GL and SC-GR points are used to approximate the solution of the VO-FFPE in space and time, respectively. The VO-FFPE is written in terms of SLP and SCP. The residuals of the VO-FFPE at the SL-GL and SC-GR quadrature points are estimated, and a system of algebraic equations is obtained and solved. Numerical results illustrated the accuracy of the procedure when solving TVO-FFPEs and TSVO-FFPEs.

References

[1] M. Abdelkawy, A. Amin and A. M. Lopes, *Fractional-order shifted Legendre collocation method for solving non-linear variable-order fractional Fredholm integro-differential equations*, Computational and Applied Mathematics, 2022, 41(1), 1–21.

[2] H. Abo-Gabal, M. A. Zaky, A. S. Hendy and E. H. Doha, *Computational aspects of fractional romanovski–bessel functions*, Computational and Applied Mathematics, 2021, 40(4), 1–16.

[3] I. G. Ameen, M. A. Zaky and E. H. Doha, *Singularity preserving spectral collocation method for nonlinear systems of fractional differential equations with the right-sided Caputo fractional derivative*, Journal of Computational and Applied Mathematics, 2021, 392, 113468.

[4] A. H. Bhrawy and M. A. Zaky, *Numerical simulation for two-dimensional variable-order fractional nonlinear cable equation*, Nonlinear Dynamics, 2015, 80(1), 101–116.

[5] A. H. Bhrawy and M. A. Zaky, *Numerical algorithm for the variable-order Caputo fractional functional differential equation*, Nonlinear Dynamics, 2016, 85(3), 1815–1823.

[6] A. H. Bhrawy and M. A. Zaky, *Highly accurate numerical schemes for multi-dimensional space variable-order fractional Schrödinger equations*, Computers & Mathematics with Applications, 2017, 73(6), 1100–1117.

[7] A. H. Bhrawy and M. A. Zaky, *An improved collocation method for multi-dimensional space–time variable-order fractional Schrödinger equations*, Applied Numerical Mathematics, 2017, 111, 197–218.

[8] C. Canuto, M. Y. Hussaini, A. Quarteroni and T. A. Zang, *Spectral Methods: Fundamentals in Single Domains*, Springer Science & Business Media, 2007.

[9] L. Chen, W. Pan, R. Wu, et al., *Design and implementation of grid multi-scroll fractional-order chaotic attractors*, Chaos: An Interdisciplinary Journal of Nonlinear Science, 2016, 26(8), 084303.

[10] Y. Chen, L. Liu, B. Li and Y. Sun, *Numerical solution for the variable order linear cable equation with Bernstein polynomials*, Applied Mathematics and Computation, 2014, 238, 329–341.

[11] Y. Chen and J. Zhou, *Error estimates of spectral Legendre–Galerkin methods for the fourth-order equation in one dimension*, Applied Mathematics and Computation, 2015, 268, 1217–1226.

[12] G. L. Delzanno, *Multi-dimensional, fully-implicit, spectral method for the Vlasov–Maxwell equations with exact conservation laws in discrete form*, Journal of Computational Physics, 2015, 301, 338–356.

[13] K. Diethelm, V. Kiryakova, Y. Luchko, et al., *Trends, directions for further research, and some open problems of fractional calculus*, Nonlinear Dynamics, 2022, 1–26.

[14] E. Doha, M. Abdelkawy, A. Amin and D. Baleanu, *Approximate solutions for solving nonlinear variable-order fractional Riccati differential equations*, Nonlinear Analysis: Modelling and Control, 2019, 24(2).

[15] E. Doha, M. Abdelkawy, A. Amin and A. M. Lopes, *A space–time spectral approximation for solving nonlinear variable-order fractional sine and Klein–Gordon differential equations*, Computational and Applied Mathematics, 2018, 37(5), 6212–6229.

[16] E. H. Doha, M. A. Abdelkawy, A. Z. Amin and A. M. Lopes, *Numerical solutions for variable-order fractional Gross–Pitaevskii equation with two spectral collocation approaches*, International Journal of Nonlinear Sciences and Numerical Simulation, 2021.

[17] E. H. Doha, M. A. Abdelkawy, A. Z. M. Amin and D. Baleanu, *Spectral technique for solving variable-order fractional volterra integro-differential equations*, Numerical Methods for Partial Differential Equations, 2018, 34(5), 1659–1677.

[18] E. H. Doha, M. A. Abdelkawy, A. Z. M. Amin and A. M. Lopes, *On spectral methods for solving variable-order fractional integro-differential equations*, Computational and Applied Mathematics, 2018, 37(3), 3937–3950.

[19] E. H. Doha, M. A. Abdelkawy, A. Z. M. Amin and A. M. Lopes, *Shifted Jacobi–Gauss-collocation with convergence analysis for fractional integro-differential equations*, Communications in Nonlinear Science and Numerical Simulation, 2019, 72, 342–359.

[20] N. A. Elkot, M. A. Zaky, E. H. Doha and I. G. Ameen, *On the rate of convergence of the Legendre spectral collocation method for multi-dimensional nonlinear Volterra–Fredholm integral equations*, Communications in Theoretical Physics, 2021, 73(2), 025002.

[21] H. Habenom and D. L. Suthar, *Numerical solution for the time-fractional Fokker-Planck equation via shifted Chebyshev polynomials of the fourth kind*, Advances in Difference Equations, 2020, 2020(1), 1–16.

[22] R. M. Hafez, S. S. Ezz-Eldien, A. H. Bhrawy, et al., *A Jacobi Gauss–Lobatto and Gauss–Radau collocation algorithm for solving fractional Fokker-Planck equations*, Nonlinear Dynamics, 2015, 82(3), 1431–1440.

[23] A. S. Hendy, M. A. Zaky, R. M. Hafez and R. H. De Staelen, *The impact of memory effect on space fractional strong quantum couplers with tunable decay behavior and its numerical simulation*, Scientific Reports, 2021, 11(1), 1–15.

[24] C. Li and A. Chen, *Numerical methods for fractional partial differential equations*, International Journal of Computer Mathematics, 2018, 95(6-7), 1048–1099.

[25] L. Pinto and E. Sousa, *Numerical solution of a time-space fractional Fokker-Planck equation with variable force field and diffusion*, Communications in Nonlinear Science and Numerical Simulation, 2017, 50, 211–228.

[26] H. Risken, *Fokker-Planck equation*, in *The Fokker-Planck Equation*, Springer, 1996, 63–95.

[27] F. Song and C. Xu, *Spectral direction splitting methods for two-dimensional space fractional diffusion equations*, Journal of Computational Physics, 2015, 299, 196–214.

[28] H. Sun, W. Chen, H. Wei and Y. Chen, *A comparative study of constant-order and variable-order fractional models in characterizing memory property of systems*, The european physical journal special topics, 2011, 193(1), 185–192.

[29] V. E. Tarasov, *Fractional fokker–planck equation for fractal media*, Chaos: An Interdisciplinary Journal of Nonlinear Science, 2005, 15(2), 023102.

[30] V. E. Tarasov, *Fokker–planck equation for fractional systems*, International Journal of Modern Physics B, 2007, 21(06), 955–967.

[31] V. E. Tarasov, *Fokker-planck equation for fractal distributions of probability*, in *Fractional Dynamics*, Springer, 2010, 123–133.

[32] V. E. Tarasov, *Fractional dynamics: applications of fractional calculus to dynamics of particles, fields and media*, Springer Science & Business Media, 2011.

[33] V. E. Tarasov, *Large lattice fractional fokker–planck equation*, Journal of Statistical Mechanics: Theory and Experiment, 2014, 2014(9), P09036.

[34] V. E. Tarasov, *Generalized memory: Fractional calculus approach*, Fractal and Fractional, 2018, 2(4), 23.

[35] V. E. Tarasov, *Applications in Physics, Part B*, De Gruyter, 2019.

[36] V. E. Tarasov, *Fractional econophysics: Market price dynamics with memory effects*, Physica A: Statistical Mechanics and its Applications, 2020, 557, 124865.

[37] V. E. Tarasov and V. V. Tarasova, *Economic dynamics with memory: Fractional calculus approach*, 8, Walter de Gruyter GmbH & Co KG, 2021.

[38] V. E. Tarasov and G. M. Zaslavsky, *Fokker–planck equation with fractional coordinate derivatives*, Physica A: Statistical Mechanics and Its Applications, 2008, 387(26), 6505–6512.

[39] D. Tavares, R. Almeida and D. F. M. Torres, *Caputo derivatives of fractional variable order: numerical approximations*, Communications in Nonlinear Science and Numerical Simulation, 2016, 35, 69–87.

[40] J. P. Ugarte, C. Tobón, A. Mendes Lopes and J. A. Tenreiro Machado, *Atrial rotor dynamics under complex fractional order diffusion*, Frontiers in physiology, 2018, 9, 975.

[41] J. Xie, Z. Yao, H. Gui, et al., *A two-dimensional Chebyshev waveletsapproach for solving the Fokker-Planck equations of time and space fractional derivatives type with variable coefficients*, Applied Mathematics and Computation, 2018, 332, 197–208.

[42] M. A. Zaky, *An accurate spectral collocation method for nonlinear systems of fractional differential equations and related integral equations with nonsmooth solutions*, Applied Numerical Mathematics, 2020, 154, 205–222.

[43] M. A. Zaky, A. S. Hendy and R. H. De Staelen, *Alikhanov Legendre—Galerkin spectral method for the coupled nonlinear time-space fractional Ginzburg–Landau complex system*, Mathematics, 2021, 9(2), 183.

[44] M. A. Zaky, A. S. Hendy and D. Suragan, *Logarithmic Jacobi collocation method for Caputo–Hadamard fractional differential equations*, Applied Numerical Mathematics, 2022, 181(1), 326–346.

[45] Z. Zhao and C. Li, *A numerical approach to the generalized nonlinear fractional Fokker-Planck equation*, Computers & Mathematics with Applications, 2012, 64(10), 3075–3089.